RESEARCH ARTICLE

JOR *Spine* OPEN ACCESS

PHLPP1 deficiency protects against age-related intervertebral disc degeneration

Changli Zhang ◉ | **Katherine M. Joseph** ◉ | **Nazir M. Khan** ◉ |
Martha Elena Diaz-Hernandez ◉ | **Hicham Drissi** ◉ | **Svenja Illien-Junger** ◉

Department of Orthopaedics, Emory University School of Medicine, Atlanta, Georgia, USA

Correspondence
Svenja Illien-Junger, Department of Orthopaedics, Emory University School of Medicine, 21 Ortho Lane, Atlanta, GA 30329, USA.
Email: svenja.illien-junger@emory.edu

Abstract

Background: Intervertebral disc (IVD) degeneration is strongly associated with low back pain and is highly prevalent in the elderly population. Hallmarks of IVD degeneration include cell loss and extracellular matrix degradation. The PH domain leucine-rich-repeats protein phosphatase (PHLPP1) is highly expressed in diseased cartilaginous tissues where it is linked to extracellular matrix degradation. This study explored the ability of PHLPP1 deficiency to protect against age-related spontaneous IVD degeneration.

Methods: Lumbar IVDs of global *Phlpp1* knockout (KO) and wildtype (WT) mice were collected at 5 months (young) and 20 months (aged). Picrosirius red–alcian blue staining (PR-AB) was performed to examine IVD structure and histological score. The expression of aggrecan, ADAMTS5, KRT19, FOXO1 and FOXO3 was analyzed through immunohistochemistry. Cell apoptosis was assessed by TUNEL assay. Human nucleus pulposus (NP) samples were obtained from patients diagnosed with IVD degeneration. *PHLPP1* knockdown in human degenerated NP cells was conducted using small interfering RNA (siRNA) transfection. The expression of PHLPP1 regulated downstream targets was analyzed via immunoblot and real time quantitative PCR.

Results: Histological analysis showed that *Phlpp1* KO decreased the prevalence and severity of age-related IVD degeneration. The deficiency of PHLPP1 promoted the increased expression of NP phenotypic marker KRT19, aggrecan and FOXO1, and decreased levels of ADMATS5 and cell apoptosis in the NP of aged mice. In degenerated human NP cells, *PHLPP1* knockdown induced FOXO1 protein levels while FOXO1 inhibition offset the beneficial effects of *PHLPP1* knockdown on KRT19 gene and protein expression.

Conclusions: Our findings indicate that *Phlpp1* deficiency protected against NP phenotypic changes, extracellular matrix degradation, and cell apoptosis in the process of IVD degeneration, probably through FOXO1 activation, making PHLPP1 a promising therapeutic target for treating IVD degeneration.

KEYWORDS
aging, FOXO1, intervertebral disc degeneration, matrix homeostasis, nucleus pulposus, PHLPP1

1 | INTRODUCTION

Back pain is a leading cause of physical disability worldwide and its socioeconomic impact increases exponentially as the global population ages.[1,2] Intervertebral disc (IVD) degeneration is the most common cause of back pain in older adults.[3] As the largest avascular organ in the body, the IVD has limited self-repair capabilities, causing increased severity of IVD degeneration over time.[4] The causes for IVD degeneration are multifactorial and include risk factors such as trauma, heritability, repetitive overloading, and aging.[5–9] Age-related IVD degeneration is characterized by a catabolic shift, chronic inflammation, cell death, and extracellular matrix (ECM) degradation.[10,11] The proteoglycan-rich and hydrated nucleus pulposus (NP) matrix becomes collagen-dominated and fibrous.[12] Notochordal cells are replaced by chondrocyte-like cells and the number of apoptotic cells in the IVD increases.[13] In addition to the cellular and ECM alterations, proinflammatory cytokines are upregulated in degenerated IVDs, contributing to matrix breakdown by enhancing the expression of matrix metalloproteinases (MMPs), a disintegrin and metalloprotease with thrombospondin motif (ADAMTS), and inhibiting the synthesis of matrix molecules.[14–16] As the IVD ages, the expression of the NP phenotypic marker Cytokeratin 19 (KRT19) and the FOXO transcription factors decrease, which has been correlated with increased IVD degeneration.[17,18]

The Ser/Thr protein phosphatase PH domain Leucine-rich-repeats protein phosphatase 1 (PHLPP1) regulates several kinases involved in cell survival and apoptosis, autophagy, differentiation, inflammation, and matrix catabolism,[19–22] including protein kinase B (AKT),[23] protein kinase C (PKC),[24] mammalian sterile 20-like kinase 1 (MST1)[25] and ribosomal protein S6 kinase (S6K1).[26] Genetic depletion of *Phlpp1* in mice protects against osteoarthritis progression,[27] suppresses intestinal epithelial cell apoptosis,[28] and provides cardio protection via AKT signaling.[29] We previously demonstrated that PHLPP1 expression positively correlates with human IVD degeneration and that its deficiency in mice promotes healing from needle puncture injury by concurrently increasing IVD matrix production and cellularity and reducing cell apoptosis in mice.[30]

However, spontaneous development of IVD degeneration, not injury or trauma, is the main risk factor for the high prevalence of IVD degeneration. The aim of this study was to first, determine if *Phlpp1* deficiency can delay the progression of spontaneous IVD degeneration by suppressing matrix degradation and cell apoptosis in aged mice and second, if *PHLPP1* knockdown can promote NP cell regeneration of human degenerated NP cells from older patients. Lumbar IVDs from global *Phlpp1* KO and WT mice were examined through histology, immunohistochemistry and TUNEL assay at 5 and 20 months. *PHLLP1* knockdown in human degenerated NP cells was conducted using small interfering RNA transfection.

2 | MATERIALS AND METHODS

2.1 | Mouse model

All animal research was conducted in accordance with the recommendations stated in the Guide for the Care and Use of Laboratory Animals of the National Institutes of Health (U.S. Department of Health, Education, and Welfare, NIH 78-23, 1996). All animal protocols were approved by the Atlanta Veteran's Affairs Medical Center's Institutional Animal Care and Use Committee (Protocol V016-19). C57BL/6J mice and PHLPP1 KO mice were sacrificed at 5 (WT: $n = 4$, one female and three males; KO: $n = 4$, two females and two males) and 20 (WT: $n = 11$, five females and six males; KO: n = 13, eight females and five males) months of age. Lumbar IVDs (L3–L6) were isolated and used for downstream analysis.

2.2 | Histology and immunochemistry

IVDs were fixed in z-fix (Sigma Aldrich, Z2902-3.75L) for 2 days and decalcified in 5% Formic acid (Millipore Sigma, FX0440-6) for 3 days. Decalcified IVDs were embedded in paraffin and 5 μm thick midsagittal sections were used for histology and immunochemistry. IVD morphology was visualized using Picrosirius red–alcian blue staining (PR-AB).

For immunohistochemistry, antigen retrieval was performed by applying 0.8% hyaluronidase (Sigma Aldrich, H3506) for 1 h at 37°C, followed by a 30-minute incubation in 2.5% normal horse serum for blocking (ImmPress–AP Horse Anti-Rabbit IgG Polymer Reagent, MP- 5401-50, Vector Laboratories). Samples were then incubated with primary antibodies against ADAMTS5 (ab41037, ABCAM), aggrecan (BS-1223R, Bioss), KRT19 (TROMA-III, DSHB), FOXO1 (2880, cell signaling) and FOXO3a (2497, cell signaling). After overnight incubation at 4°C, the samples were washed and incubated with an alkaline phosphatase conjugated secondary antibody (ImmPress–AP Horse Anti-Rabbit IgG Polymer Reagent, MP-5401-50, Vector Laboratories) for 30 min and visualized using alkaline phosphatase substrate (SK-5105 ImmPACT Vector Red, Vector Laboratories). For KRT19 immunostaining, the samples were treated with peroxidase suppressor (35 000, Thermo Fisher) for 30 min after primary antibody incubation, and then incubated with Signal Stain Boost IHC detection reagent (8125, cell signaling). All samples were counterstained with Mayer's hematoxylin and mounted. Universal negative control serum (NC498, BioCare Medical) was used as negative control. Sections were imaged using a bright-field microscopy (DM6 B automated microscope with LAS X software, Leica, Germany). One section per animal was obtained and the immunopositively areas/cells were quantified in the whole NP by two independent observers who were blinded to experimental groups.

2.3 | TUNEL assay

TUNEL assay was performed following the manufacture's protocol (C10618, Thermo Fisher). In brief, 5 μm thick midsagittal sections were deparaffinized, dehydrated, and permeabilized in proteinase K solution for 15 min at room temperature. Samples were then incubated with TUNEL reaction mixture in a humidified atmosphere for 1 h at 37°C. Sections were mounted with antifade mounting medium with DAPI (H1200, Vector laboratories) and visualized using a

TABLE 1 Human IVD donors

Patient	Gender	Age (years)	IDD grade
1	M	74	5
2	M	61	5
3	M	61	5
4	F	72	4

fluorescence microscope (DM6 B automated microscope with LAS X software, Leica, Germany). One section per animal was obtained and the percentage of TUNEL-positive cells in both NP and AF tissues was qualified in Image J by two independent observers who were blinded to experimental groups.

2.4 | Human NP cell extraction and culture

Following informed consent in accordance with the institutional review board approval, four human NP tissues were obtained from patients with discogenic pain and graded by surgeons as Grade IV or V on the Pfirrmann scale (Table 1).[31] Immediately after surgery, the specimens were washed with five dips of 70% Ethanol, $1\times$ PBS with 3% pen/strep and 1.5% Amphotericin B, and $1\times$ PBS to prevent contamination. NP tissues were minced into small fragments ($\sim$1 mm^3).Cells were released from the tissues by digestion in 0.2% protease (Sigma Aldrich, P5147-1G) for 1 h, followed by 0.025% collagenase P (Roche Diagnostics, 40 341 623) digestion for 4 h. Isolated cells were filtered through 100-μm mesh and rinsed twice with $1\times$ PBS. NP cells were expanded in low glucose DMEM containing 10% premium fetal bovine serum (FBS), 1% pen/strep, 1% primocin, and 50 μg/ml ascorbate. All cells were grown at 37°C under 5% CO_2, 20% O_2, and 90% humidity. Culture medium was changed every other day. Cells of passage 2–3 were used for experiments.

2.5 | Cell transfection

Human degenerated NP cells were seeded in 12-well plate until reaching 70% of confluence. Cells were transiently transfected with 20 nM ON-TARGET plus *PHLPP1* siRNA SMARTPool (L-019103-00-0005, Horizon, UK), or control siRNA (D-001810-01-05, Horizon, UK). For all the transfections, Dharma FECT1 transfection reagent (T-2002-01, Horizon, UK) was used by mixing with siRNA for 30 min at room temperature. To minimize cell toxicity induced by transfection, transfection media was removed after 24 h, and normal culture media was added. Cells were cultured for another 48 h and then harvested for protein extraction.

2.6 | RNA isolation and reverse transcription-quantitative PCR

RNA was extracted using TRIzol reagent (Thermofisher Scientific, 15 596 026) and chloroform (Thermofisher Scientific, AAJ67241AP),

followed by RNeasy micro kit (Qiagen, 74 004) according to manufacturer's instructions. RNA concentration and purity were determined using NanoDrop 2000 spectrophotometers (Thermofisher Scientific, ND-2000). For mRNA, 1 μg of RNA was used for reverse transcription into cDNA using Supersript VILO cDNA synthesis kit (Thermofisher Scientific, 11 754 050). For each quantitative PCR reaction, 5 ng cDNA was mixed with Taqman primers (*KRT19*: Hs01051611_gH and *GAPDH*: Hs02758991_g1), $2\times$ Taqman universal PCR master mix (Thermofisher Scientific, 4 304 437), and RNAse-free water to a total volume of 20 μl. Gene expression was measured with the Rotor-Gene Q detection system (Qiagen). *GAPDH* was used for the endogenous control. Fold change of *KRT19* gene expression was calculated using $2^{-\Delta\Delta Ct}$ method.

2.7 | Inhibitor treatment

The 100 nM FOXO1 inhibitor AS1842856 (Millipore Sigma, 344 355) or 100 nM PI3K/AKT inhibitor Wortmannin (Millipore Sigma, W1628) were dissolved in DMSO. To collect cells for RNA, degenerated human NP cells were transfected for 24 h, followed by FOXO1 inhibitor stimulation for another 24 h. To collect cells for protein, NP cells were transfected for 48 h and then stimulated with FOXO1 inhibitor for 24 h. An equivalent amount of DMSO was used in the untreated group.

2.8 | Immunoblot analysis

Whole-cell extracts were isolated from human degenerated NP cells followed by lysis in RIPA buffer (Millipore Sigma, R0278) containing freshly added protease inhibitor cocktail (Thermofisher Scientific, 78 430). Protein concentration was determined by Bicinchoninic Acid assay (Thermofisher Scientific, J23227) using bovine serum albumin as the standard. Equal amounts of protein (20 μg) were loaded onto gradient gels (4%–20%, precast SDS-PAGE gels [BioRad, 4 561 094]), and transferred to PVDF membrane (BioRad, 1 620 177). The membrane was blocked with 5% Milk/TBS-T buffer for 1 h and then incubated with primary antibodies against PHLPP1 (Sigma-Aldrich, 071341), Phospho-AKT Ser473 (Cell Signaling Technology, 9271), AKT (Cell Signaling Technology, 9272), phospho-p44/42 MAPK ERK1/2 (Cell Signaling Technology, 9101), p44/42 MAPK ERK1/2 (Cell Signaling Technology, 9102), FOXO1 (Cell Signaling Technology, 2880S), FOXO3a (Cell signaling, 2497), KRT19 (TROMA-III, DSHB) or GAPDH (Cell Signaling Technology, 884S). All antibodies were diluted at 1:1000. After overnight incubation with primary antibodies at 4°C, membranes were washed in TBST and incubated with horseradish peroxidase (HRP)-conjugated secondary antibody (1:5000, Cell Signaling Technology, 7074S) or mouse HRP (1:5000, Cell Signaling Technology, 7076S) for 1 h. Membranes incubated with GAPDH were imaged directly after washing with TBST. Protein bands were visualized using Amersham ECL select western blotting detection reagent (VWR, 89233-310) and iBright FL 1500 imaging system (Thermo Fisher). Band densities were calculated using image J.

2.9 | Statistics

Two-way analysis of variance (ANOVA) testing was utilized to assess the effect of aging, genotype, and sex on IVD degeneration (Table A1). Because sex was not identified as significant variable, sexes were combined and two-way ANOVAs were utilized to analyze differences between genotypes and age, with subsequent Bonferroni post hoc testing. Power analysis was performed using G*Power to determine the sample size (using a significance level of 0.05 and a power of 0.8). Human data were analyzed by t tests (knockdown experiments) or one-way ANOVAs, followed by Bonferroni post hoc testing (inhibitor treatment). The statistical analyses were performed using GraphPad Prism9 (GraphPad Software, Inc., La Jolla, CA). A p value <0.05 was considered statistically significant.

3 | RESULTS

3.1 | *Phlpp1* deficiency alleviated age-related spontaneous IVD degeneration in IVDs of aged mice

To investigate if *Phlpp1* depletion is protective against spontaneous IVD degeneration in aged mice, we analyzed IVDs of lumbar spines from both WT and KO mice at (5-young and 20-months old) of age, corresponding to the ages with low (20–30 years) and high (50–60 years) prevalence of IVD degeneration in humans.[32,33] Picrosirius red-alcian blue staining (PR-AB) was performed to assess the alterations of IVD compartment organization and matrix composition. We quantified histopathological changes using a previously established histological grading system.[34] The IVD degeneration score for each IVD is listed in Table A2. In young mice, no detectable differences were observed in the IVD structure and proteoglycan accumulation in WT and KO IVDs. All mice displayed a typical healthy IVD structure, consisting of a central notochordal NP cell band embedded in pronounced proteoglycans, which surrounded by the highly organized collagenous matrix of the annulus fibrosus (AF, Figure 1A).Compared to young WT and agedKO IVDs, the occurrence of IVD degeneration in agedWT mice was significantly increased (Figure 1B–D; Table 2). We observed that 75% of agedWT IVDs were degenerated, while only 33% of KO IVDs showed degenerative changes. In addition to the lower incidence of IVD degeneration, agedKO IVDs displayed less severe degenerative features. Specifically, 21% of the degenerated IVDs in agedWT
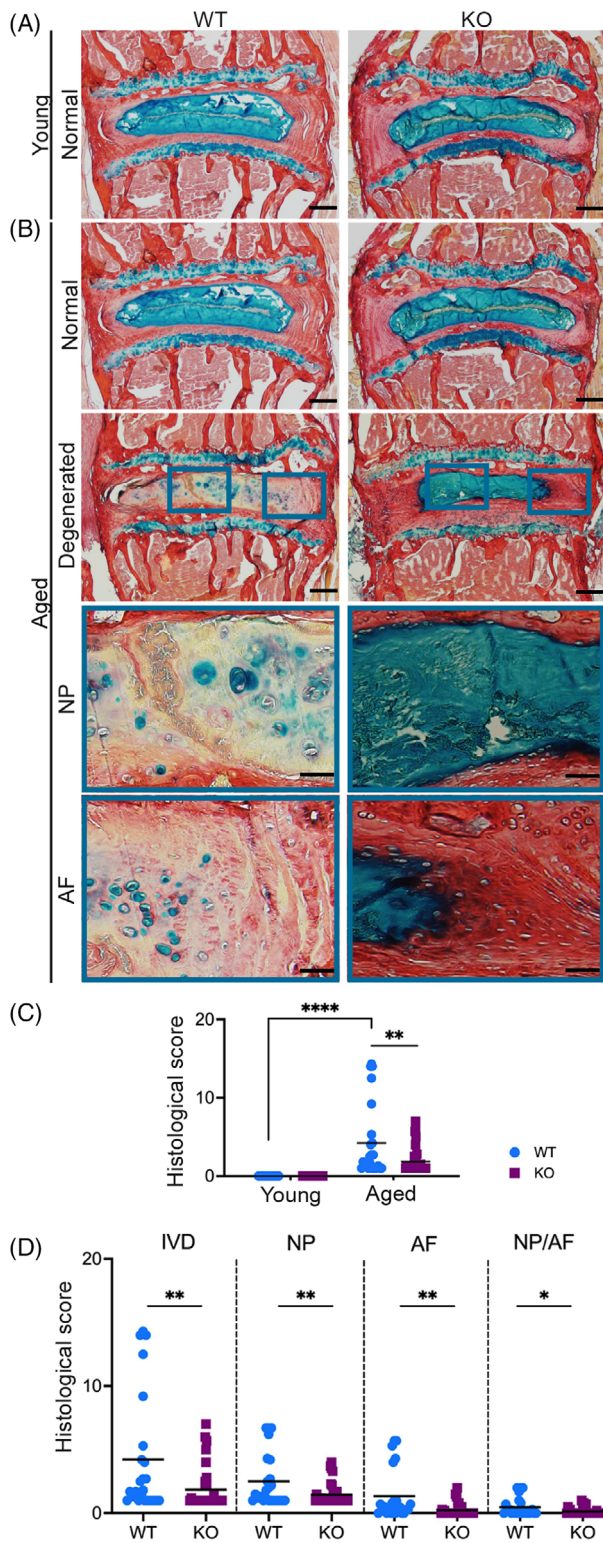
FIGURE 1 PHLPP1 deficiency decelerated age-related spontaneous IVD degeneration. (A–C) Pirco-sirius red/alcian blue (PRAB) staining of WT and KO IVDs. (A) No obvious differences in IVD structure were detected between young and aged mice. (B) Severely degenerated IVDs of agedWT mice (left) displayed chondrocyte-like cells scattered in fibrocartilaginous matrix with less alcian blue stain in the NP. Only mild degeneration was observed in KO IVDs and proteoglycans were preserved in all KO IVDs (right). Blue boxes indicate regions of interest. (C) Quantification of histological scores. (D) Contribution of NP, AF and NP/AF boundary to histological scorings of aged mouse IVDs. Data are represented as mean $+/-$ SD. Young: $n = 12$ IVDs/genotype; AgedWT: $n = 23$ IVDs; AgedKO: n = 30 IVDs. Scale bar = 200 μm and 50 μm (insert). *$p < 0.05$. **$p < 0.01$. ****$p < 0.0001$

groups were severely degenerated (Table 3), which is characterized by a complete replacement of notochordal NP cells with hypertrophic chondrocytes, the formation of fibrocartilaginous matrix and clefts, and loss of discernable AF/NP boundaries (Figure 1B, left).

TABLE 2 Incidence of IVD degeneration in young and aged mice

Number of IDD (%)			
		WT	KO
Young	Mice	0 (0%)	0 (0%)
	IVDs	0 (0%)	0 (0%)
Aged	Mice	11 (100%)	10 (72%)
	IVDs	18 (75%)	11 (33%)

TABLE 3 Incidence of severe IVD degeneration in young and aged mice

Number of severe IDD (%)			
		WT	KO
Young	Mice	0 (0%)	0 (0%)
	IVDs	0 (0%)	0 (0%)
Aged	Mice	3 (27%)	0 (0%)
	IVDs	5 (21%)	0 (0%)

None of these severe degenerative features were detected in IVDs from agedKO mice, which all maintained high NP proteoglycan deposition (Figure 1B, right). The improvement of histological features in agedKO mice was also demonstrated by the distribution of histological scores in each compartment (Figure 1D). Taken together, our findings suggest that *Phlpp1* deficiency maintained a higher proteoglycan content and decreased both the prevalence and severity of spontaneous IVD degeneration in aged mouse IVDs.

3.2 | *Phlpp1* deficiency protected against aggrecan degradation in aged mice

Aggrecan is the main proteoglycan in the NP and an important component for proper mechanical and structural function of IVDs.[35] We performed immunostaining to determine whether *Phlpp1* depletion maintained aggrecan deposition in NPs of agedKO mice. Consistent with the decrease of proteoglycans evidenced from PR-AB staining, aggrecan deposition was reduced in agedWT IVDs, where severely degenerated IVDs rarely expressed any aggrecan (Figure 2A–D). In contrast, aged IVDs from KO mice maintained aggrecan content at levels similar to youngKO mice, which were significantly higher compared to agedWT IVDs (Figure 2A–D).
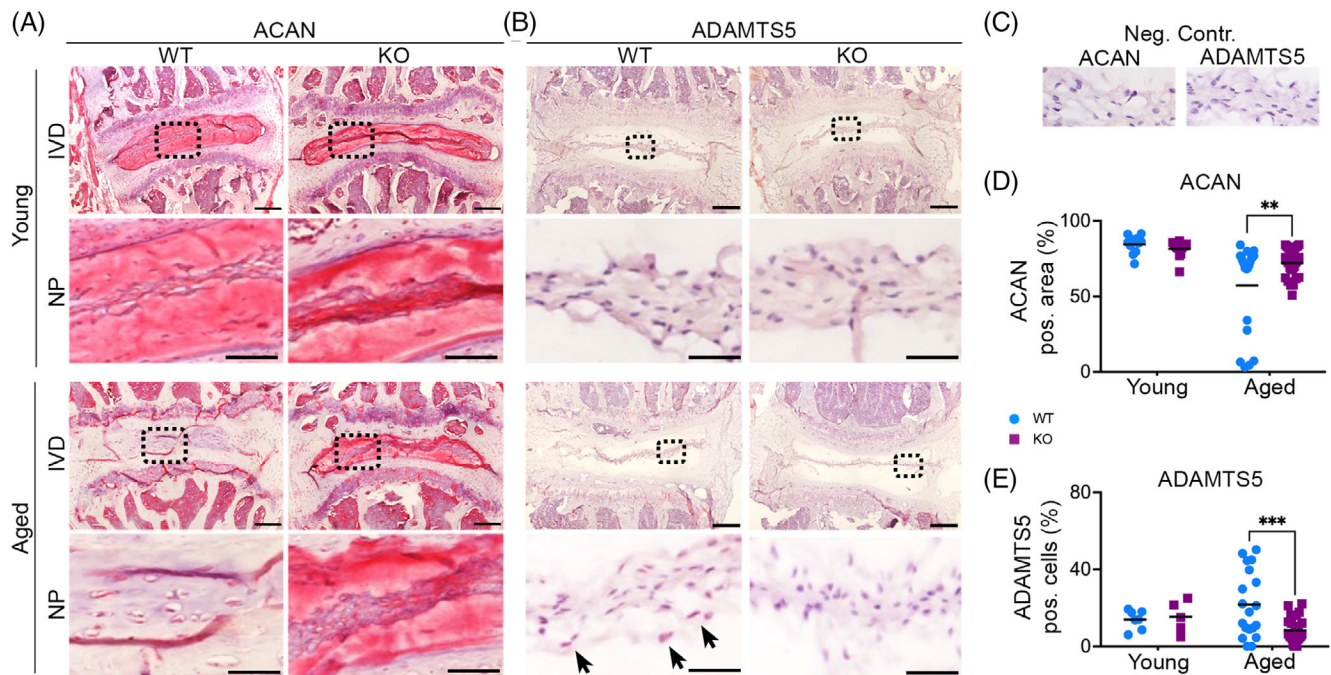
FIGURE 2 PHLPP1 deficiency protected against aggrecan degradation in aged IVDs. Representative images of (A) aggrecan (B) and ADAMTS5 immunostaining of young and aged mice. Positive immunosignal is stained with red. Arrows indicate positive cells. Lower panel shows the magnified area in the black box. (C) Quantification of aggrecan. Young WT and KO IVDs showed comparable aggrecan expression. AgedKO IVDs displayed more aggrecan expression than agedWT IVDs. (D) Quantification of ADAMTS5 immunopositivity. ADAMTS5 expression did not show obvious differences in the NP of young mice, but ADAMTS5 was increased in agedWT compared to agedKO NPs. Red = aggrecan and ADAMTS5, Purple = hematoxylin counterstain; Scale bar = 200 μm and 50 μm (insert). Data are represented as mean +/− SD. Young: $n = 12$ IVDs/genotype; AgedWT: $n = 23$ IVDs; AgedKO: $n = 30$ IVDs. **$p < 0.01$. ***$p < 0.001$
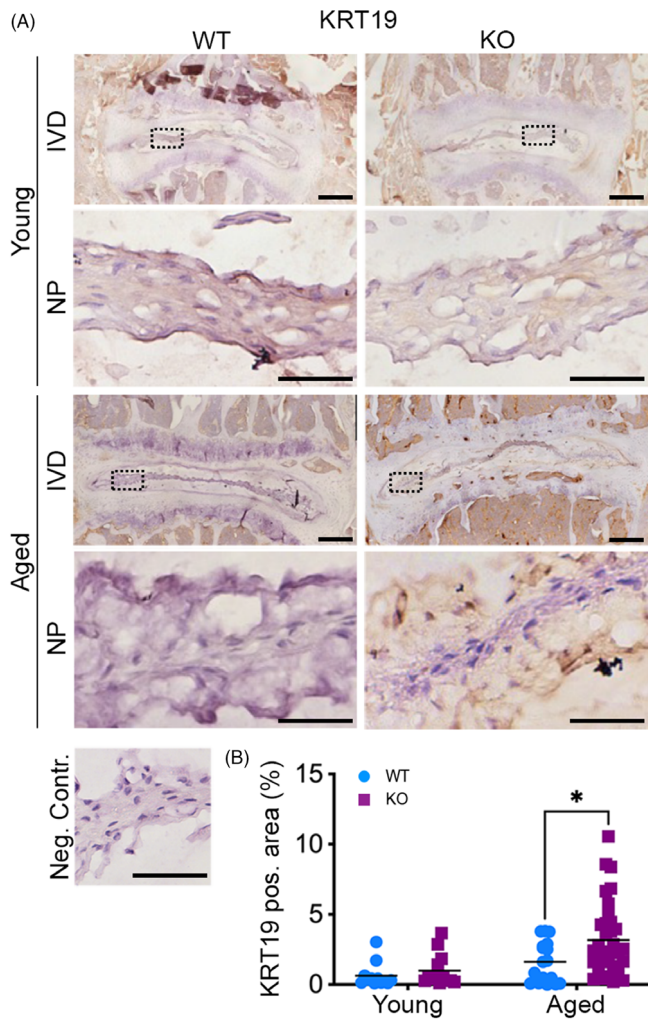
FIGURE 3 PHLPP1 deficiency promoted the expression of NP phenotypic maker KRT19. (A) Representative images of immunostaining for KRT19 in the NP of young and agedWT and PHLPP1 KO mice. Lower panel shows the magnified area in the black box. (B) Quantification of KRT19 immunostaining. The expression of KRT19 in the NP was increased in the NP of agedKO mice compared to agedWT mice. Brown = KRT19, Purple = hematoxylin counterstain; Scale bar = 200 μm; insert scale bar = 50 μm. Data are represented as mean $+/-$ SD. Young: $n = 12$ IVDs/genotype; AgedWT: $n = 23$ IVDs; AgedKO: $n = 30$ IVDs. *$p < 0.05$

FIGURE 4 PHLPP1 deficiency protected against cell apoptosis in aged IVDs. (A) Representative images of TUNEL assay of the NP in young and agedWT and KO mice. (B) Quantification of TUNEL assay. Apoptotic cells were decreased in agedKO compared to WT IVDs. Red = apoptotic cells, Blue = nuclei. Scale bar = 200 μm and 50 μm (insert). Data are represented as mean $+/-$ SD. Young: $n = 12$ IVDs/genotype; AgedWT: $n = 23$ IVDs; AgedKO: $n = 30$ IVDs.*$p < 0.05$

The aggrecanase ADAMTS5 is one of the key mediators of aggrecan degradation in the NP.[36] Only minor ADAMTS5 expression was observed in the NP of youngWT and KO mice which was maintained at low levels in agedKO mice (Figure 2B–E).In contrast, its expression was significantly increased in the NP of agedWT mice and was significantly higher compared to KO mice (Figure 2B–E). Collectively, these results indicate that *Phlpp1* depletion maintained aggrecan deposition in the NP of agedKO mice, partially by protecting against aggrecan degradation through repression of ADAMTS5.

3.3 | *Phlpp1* deficiency increased the expression of NP phenotypic marker KRT19 in aged IVDs

To examine if the enhanced matrix deposition and reduced degenerative changes were accompanied by a healthier NP phenotype, we immunohistochemically assessed the level of the NP phenotypic marker KRT19 (Figure 3). KRT19 expression patterns confirmed the
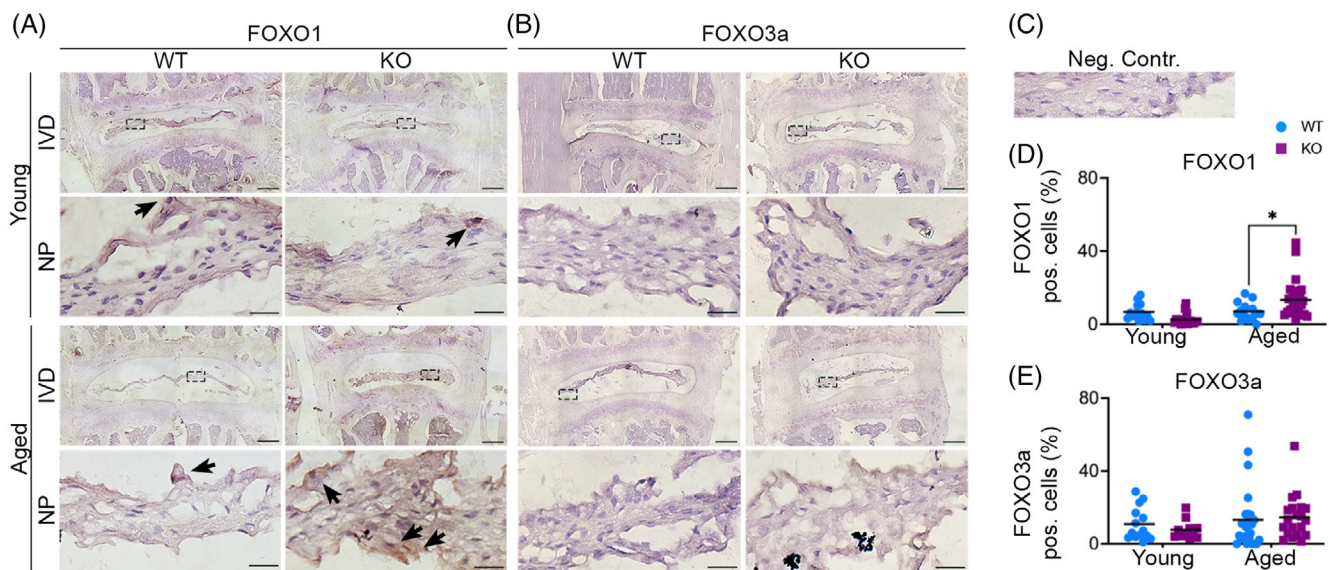
FIGURE 5   PHLPP1 deficiency promoted the expression of FOXO1 in aged mouse NPs. Representative images of (A) FOXO1 and (B) FOXO3a immunostaining in the NPs of young and aged mice. Black boxes indicate the magnified NP area. (C) Negative controls. (D) Quantification of FOXO1 immunostaining. The expression of FOXO1 was increased in agedKO compared to WT IVDs. (E) Quantification of FOXO3a immunostaining. The expression of FOXO3a in the NP was comparable between young and agedWT and KO mice. Brown = FOXO1 and FOXO3a positive signal, Purple = hematoxylin counterstain; Scale bar = 200 μm and 50 μm (insert). Data are represented as mean $+/-$ SD. Young: $n = 12$ IVDs/genotype; AgedWT: $n = 23$ IVDs; AgedKO: $n = 30$ IVDs.*$p < 0.05$

protective effect of *Phlpp1* depletion on NP tissues in agedKO mice. Specifically, no changes in the expression of KRT19 were detected in young IVDs between two genotypes, but its expression significantly increased in the NP of agedKO compared to agedWT IVDs, potentially as a response to the worsening microenvironment in the aging NP.

3.4 | *Phlpp1* deficiency protected against cell apoptosis in aged IVDs

Apoptosis is yet another hallmark of IVD degeneration during aging.[13] To investigate the effects of PHLPP1 on cell apoptosis, TUNEL assays were performed on IVDs of young and agedWT and KO mice. As expected, apoptosis rates were low in the NPs of young WT and KO mice (Figure 4A) and were maintained at low levels in agedKO mice (Figure 3B, right). When compared to young mice and to agedKO mice, apoptosis was significantly increased in the NP in agedWT mice (Figure 4C), further suggesting a protective effect of *Phlpp1* KO on spontaneous IVD degeneration during aging.

3.5 | PHLPP1 deficiency promoted the expression of transcription factor FOXO1 in aged IVDs

It has recently been demonstrated that FOXOs are important players in modulating IVD homeostasis and that FOXO deficiency induced degenerative features in mouse IVDs.[37] FOXOs are under indirect control of PHLPP1.[38,39] To investigate the impact of PHLPP1 on the expression of FOXO1 and FOXO3a in aged mice, we performed

immunohistochemistry on young and agedWT and KO mice. Young WT and KO mice did not show significant differences in FOXO1 or FOXO3a expression in the NP (Figure 5A,B). However, a significant increase in the expression of FOXO1 was observed in agedKO compared to WT mice (Figure 5D), while no differences were observed in FOXO3a expression (Figure 5E). These results suggest that Phlpp1 deficiency promoted FOXO1 expression and may delay age-related, spontaneous IVD degeneration.

3.6 | *PHLPP1* knockdown increased protein levels of KRT19 via FOXO1 signaling in human degenerated NP cells

We transiently knocked down *PHLPP1* (KD) by siRNA-mediated transfection to determine whether *PHLPP1* silencing could induce a healthy NP phenotype in human degenerated NP cells. PHLPP1 protein levels of KD NP cells were significantly reduced compared to the degenerated NP cell control group (Figure 6A). As expected, *PHLPP1* knockdown promoted the phosphorylation of AKT, a known PHLPP1 substrate (Figure 6A). In contrast, ERK phosphorylation was not altered by *PHLPP1* knockdown (Figure 6A).

Consistent with the findings in mice, protein levels of FOXO1, but not FOXO3, increased significantly after *PHLPP1* knockdown (Figure 6A). To investigate if FOXO1 activity was increased and if FOXO1 was the downstream effector of PHLPP1, the KD NP cells were treated with FOXO1 inhibitor AS1842856 which binds to the active form of FOXO1. FOXO1 inhibition offset the beneficial effect of *PHLPP1* knockdown on *KRT19* gene expression (Figure 6B). Surprisingly, AKT inhibition with the small molecule
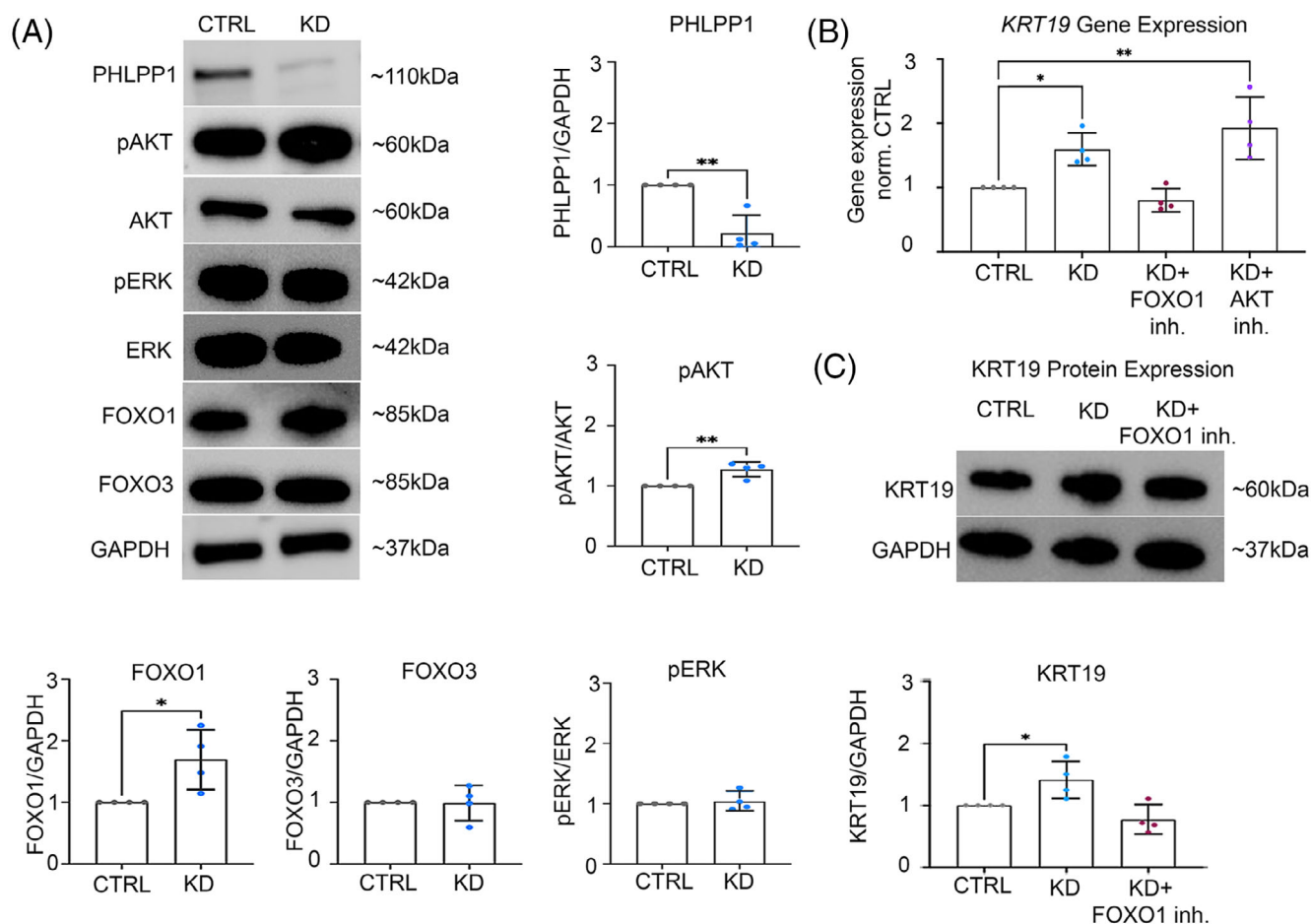
FIGURE 6 *PHLPP1* knockdown improved NP cell phenotype in degenerated human NP cells. (A) Representative immunoblots and semiquantitative analyses of PHLPP1, pAKT, AKT, pERK, ERK, FOXO1 and FOXO3a deposition in degenerated human NP cells after *PHLPP1* knockdown for 72 h. (B) KRT19 gene expression in NP cells with 24-h *PHLPP1* knockdown, followed by stimulation with FOXO inhibitor AS1842856 or PI3K/AKT inhibitor Wortmannin for another 24 h. (C) Representative immunoblots of KRT19 in NP cells with 48-hour *PHLPP1* knockdown, followed by 24-hour stimulation with FOXO inhibitor AS1842856. Degenerated NP cells with control siRNA served as control. Inh., inhibitor; KD, knockdown; Norm., normalized. Data are represented as mean $+/-$ SD. $n = 4$. *$p < 0.05$. **$p < 0.01$

PI3K/AKT inhibitor Wortmannin did not abolish *KRT19* gene expression (Figure 6B).

FOXO1 dependent KRT19 expression was further confirmed by immunoblotting. Human NP cell culture with the FOXO1 inhibitor decreased KRT19 expression in *PHLPP1* knockdown cells (Figure 6C). Taken together, these findings suggest that *PHLPP1* silencing promoted a healthy NP phenotype through targeting FOXO1 signaling, independent of AKT.

4 | DISCUSSION

This study demonstrated that PHLPP1 played a significant role in age-induced spontaneous IVD degeneration in mice and suggested a role of PHLPP1 in FOXO1 signaling in human NP cells. Our results indicated that *Phlpp1* KO maintained a healthy NP phenotype and proteoglycan content and protected against cell apoptosis while suppressing matrix degradation in aged mice. Concomitantly, suppressing the function of *PHLPP1* promoted FOXO1 activation in both aged mouse NP tissue and degenerated human NP cells. Blocking the activity of

FOXO1 abolished the beneficial effects of PHLPP1 knockdown on promoting a healthy NP cell phenotype.

Spontaneous IVD degeneration during aging is partially caused by a catabolic shift in matrix metabolism, causing progressive IVD matrix breakdown and loss of structural integrity.[40] Our data showed that systemic inhibition of PHLPP1 function improved proteoglycan deposition, specifically aggrecan deposition, reduced the expression of the matrix degradation enzyme ADAMTS5, and prevented the formation of fibrous NP tissues that occurred only in severely degenerated IVDs from aged WT mice. Anabolic effects of PHLPP1 inhibition have also been shown to be beneficial in other tissues where *Phlpp1* deficiency promoted bone formation[41] and mitigated the onset of osteoarthritis in a mouse model of osteoarthritis by increasing aggrecan and glycosaminoglycans production.[27,42]

High incidence of cell apoptosis has been reported in the IVD with age and degeneration, causing the loss of cell number and failure in replenishing the functional extracellular matrix.[43] Targeting pathways that are involved in cell apoptosis have been explored as a therapeutic approach to halt IVD degeneration.[13] Our data demonstrated that, in addition to the protective effects of PHLPP1 deficiency on maintaining proteoglycan content, apoptosis was attenuated in the NP of agedKO

mice. Inhibition of PHLPP1 function has been found to attenuate apoptosis in myocytes, intestinal epithelial cells, and neurons,[28,29,44] providing protection against tissue injuries. PHLPP1 is known to directly dephosphorylate and promote apoptotic pathways such as Mst1, and inactive pro-survival pathways such as AKT, PKC and p70S6 kinase.[24–26,45] One of the key regulators in IVD cell apoptosis is AKT signaling.[46,47] Our in vitro findings showed that *PHLPP1* knockdown increased AKT phosphorylation in human degenerated NP cells while inhibiting AKT activity did not reverse the effects of PHLPP1 knockdown on *KRT19* gene expression. It is possible that AKT signaling is not involved in promoting NP phenotype, but regulating cell survival in the IVD. These findings, together with our data on apoptosis, suggest that PHLPP1 is a potential target for preventing cell loss in IVD degeneration.

Recent studies found that deletion of FOXOs caused accelerated IVD degeneration in aged mice which was accompanied by severe cell loss in the NP and endplate.[37] Our data in mice demonstrated that *Phlpp1* KO promoted FOXO1 expression in mouse NP tissue, and that silencing *PHLPP1* in degenerated human NP cells promoted a healthy NP cell phenotype by increasing FOXO1 expression. Inhibiting FOXO1 function abolished the *PHLPP1* knockdown induced expression of the NP phenotypic marker KRT19. Liu etal. demonstrated in NP cells that FOXOs expression can suppress matrix degradation induced by oxidative stress.[48] In human meniscus cells, FOXO1 overexpression rescued expression of matrix related genes.[49] In mouse meniscus, FOXOs depletion accelerated age-related damage by suppressing the expression of genes related to autophagy, antioxidant defense, and meniscus phenotype.[37] On the contrary, Bradley etal. demonstrated that *Phlpp1* deficiency promoted chondrocyte proliferation by inhibiting FOXO1 activity.[50] These contradicting results demonstrate that PHLPP1 and FOXO1 activities are complex and highly tissue dependent. Becerra etal. revealed that FOXO3a regulated PHLPP1 expression in chondrocytes.[51] However, in our study, we did not observe any relationship between FOXO3a and PHLPP1. It should also be noted that the levels of FOXO3a and FOXO1 were determined from the whole NP cell extract. Therefore, it may mask the effect of PHLPP1 on FOXO3a activity in human NP cells. Further investigation on delineating the mechanisms between FOXO1/3a and PHLPP1 during IVD degeneration is warranted.

Our study used mice with global *Phlpp1* knockout. It cannot be excluded that the surrounding tissues contributed to the delayed age-related spontaneous IVD degeneration. Contrary to observations in other tissues, where systemic PHLPP1 deficiency displayed thicker articular cartilage in young mice,[27,50] we did not observe any morphological differences between young WT and KOmouse IVDs. One reason might be that IVD cells are quiescent and therefore only display minor PHLPP1 activity in young and undegenerated IVDs.

In summary, our data demonstrated conclusively that inhibition of PHLPP1 function promoted healthier IVD histological features and prevented severe IVD degeneration in aged mice. *Phlpp1* depletion suppressed apoptosis and matrix degradation and promoted KRT19 expression, potentially via FOXO1 activation. The improved histological, immunohistochemical, and apoptotic outcomes of its depletion indicate PHLPP1 as a potential therapeutic target for treating IVD degeneration.

AUTHOR CONTRIBUTIONS

Changli Zhang–study design, data collection and analysis, manuscript creation and editing. Katherine M. Joseph–IHC processing, image acquisition, data analysis, and manuscript editing. Nazir M. Khan–study design, data interpretation, critical suggestions, and manuscript review. Martha Elena Diaz-Hernandez–human specimen collection, data interpretation, critical suggestions, manuscript review. Hicham Drissi–study design, data interpretation, critical suggestions, manuscript review. Svenja Illien-Junger–study design, data analysis, graphic designs, manuscript review and editing, and fund acquisition. All authors have read and approved the final manuscript.

CONFLICT OF INTEREST

The authors have no conflict of interest associated with this work.

ORCID

Changli Zhang https://orcid.org/0000-0002-1170-0374
Katherine M. Joseph https://orcid.org/0000-0002-0160-9518
Nazir M. Khan https://orcid.org/0000-0002-1637-7641
Martha Elena Diaz-Hernandez https://orcid.org/0000-0003-0225-981X
Hicham Drissi https://orcid.org/0000-0002-3322-281X
Svenja Illien-Junger https://orcid.org/0000-0001-9895-0693

REFERENCES

1. Hurwitz EL, Randhawa K, Yu H, Côté P, Haldeman S. The global spine care initiative: a summary of the global burden of low back and neck pain studies. *Eur Spine J.* 2018;27:796-801.
2. Vos T, Allen C, Arora M. Global, regional, and national incidence, prevalence, and years lived with disability for 310 diseases and injuries, 1990-2015: a systematic analysis for the global burden of disease study 2015. *Lancet.* 2016;388:1545-1602.
3. Podichetty VK. The aging spine: the role of inflammatory mediators in intervertebral disc degeneration. *Cell Mol Biol (Noisy-le-Grand).* 2007;53:4–18.
4. Wang F, Cai F, Shi R, Wang XH, Wu XT. Aging and age related stresses: a senescence mechanism of intervertebral disc degeneration. *Osteoarthr Cartil.* 2016;24:398-408.
5. Livshits G, Popham M, Malkin I, et al. Lumbar disc degeneration and genetic factors are the main risk factors for low back pain in women: the UK twin spine study. *Ann Rheum Dis.* 2011;70:1740-1745.
6. Nasto LA, Wang D, Robinson AR, et al. Genotoxic stress accelerates age-associated degenerative changes in intervertebral discs. *Mech Ageing Dev.* 2013;134:35-42.
7. Elfering A, Semmer N, Birkhofer D, Zanetti M, Hodler J, Boos N. Risk factors for lumbar disc degeneration: a 5-year prospective MRI study in asymptomatic individuals. *Spine.* 2002;27:125-134.
8. Walter BA, Korecki CL, Purmessur D, Roughley PJ, Michalek AJ, Iatridis JC. Complex loading affects intervertebral disc mechanics and biology. *Osteoarthr Cartil.* 2011;19:1011-1018.
9. Vo NV, Hartman RA, Patil PR, et al. Molecular mechanisms of biological aging in intervertebral discs. *J Orthop Res.* 2016;34:1289-1306.

10. Gruber HE, Hanley EN. Analysis of aging and degeneration of the human intervertebral disc. Comparison of surgical specimens with normal controls. *Spine*. 1998;*23*:751-757.

11. Buckwalter JA. Aging and degeneration of the human intervertebral disc. *Spine*. 1995;*20*:1307-1314.

12. Patel KP, Sandy JD, Akeda K, et al. Aggrecanases and aggrecanase-generated fragments in the human intervertebral disc at early and advanced stages of disc degeneration. *Spine*. 2007;*32*:2596-2603.

13. Ding F, Shao Z, Xiong L. Cell death in intervertebral disc degeneration. *Apoptosis*. 2013;*18*:777-785.

14. Weber KT, Alipui DO, Sison CP, et al. Serum levels of the proinflammatory cytokine interleukin-6 vary based on diagnoses in individuals with lumbar intervertebral disc diseases. *Arthritis Res Ther*. 2016;*18*:3.

15. Risbud MV, Shapiro IM. Role of cytokines in intervertebral disc degeneration: pain and disc content. *Nat Rev Rheumatol*. 2014;*10*:44-56.

16. Le Maitre CL, Hoyland JA, Freemont AJ. Catabolic cytokine expression in degenerate and herniated human intervertebral discs: IL-1beta and TNFalpha expression profile. *Arthritis Res Ther*. 2007;*9*:R77.

17. Alvarez-Garcia O, Matsuzaki T, Olmer M, Masuda K, Lotz MK. Age-related reduction in the expression of FOXO transcription factors and correlations with intervertebral disc degeneration. *J Orthop Res*. 2017;*35*:2682-2691.

18. Minogue BM, Richardson SM, Zeef LA, Freemont AJ, Hoyland JA. Transcriptional profiling of bovine intervertebral disc cells: implications for identification of normal and degenerate human intervertebral disc cell phenotypes. *Arthritis Res Ther*. 2010;*12*:R22.

19. Newton AC, Trotman LC. Turning off AKT: PHLPP as a drug target. *Annu Rev Pharmacol Toxicol*. 2014;*54*:537-558.

20. Teng D-C, Sun J, An YQ, et al. Role of PHLPP1 in inflammation response: its loss contributes to gliomas development and progression. *Int Immunopharmacol*. 2016;*34*:229-234.

21. Baffi TR, Cohen-Katsenelson K, Newton AC. Phlpping the script: emerging roles of PHLPP phosphatases in cell signaling. *Annu Rev Pharmacol Toxicol*. 2021;*61*:723-743.

22. Arias E, Sandy JD, Akeda K, et al. Lysosomal mTORC2/PHLPP1/Akt regulate chaperone-mediated autophagy. *Mol Cell*. 2015;*59*:270-284.

23. Gao T, Furnari F, Newton AC. PHLPP: a phosphatase that directly dephosphorylates Akt, promotes apoptosis, and suppresses tumor growth. *Mol Cell*. 2005;*18*:13-24.

24. Gao T, Brognard J, Newton AC. The phosphatase PHLPP controls the cellular levels of protein kinase C. *J Biol Chem*. 2008;*283*:6300-6311.

25. Qiao M, Wang Y, Xu X, et al. Mst1 is an interacting protein that mediates PHLPPs' induced apoptosis. *Mol Cell*. 2010;*38*:512-523.

26. Liu J, Stevens PD, Li X, Schmidt MD, Gao T. PHLPP-mediated dephosphorylation of S6K1 inhibits protein translation and cell growth. *Mol Cell Biol*. 2011;*31*:4917-4927.

27. Bradley EW, Carpio LR, McGee-Lawrence ME, et al. Phlpp1 facilitates post-traumatic osteoarthritis and is induced by inflammation and promoter demethylation in human osteoarthritis. *Osteoarthr Cartil*. 2016;*24*:1021-1028.

28. Wen Y-A, Li X, Goretsky T, Weiss HL, Barrett TA, Gao T. Loss of PHLPP protects against colitis by inhibiting intestinal epithelial cell apoptosis. *Biochim Biophys Acta*. 2015;*1852*:2013-2023.

29. Miyamoto S, Purcell NH, Smith JM, et al. PHLPP-1 negatively regulates Akt activity and survival in the heart. *Circ Res*. 2010;*107*:476-484.

30. Zhang C, Smith MP, Zhou GK, et al. Phlpp1 is associated with human intervertebral disc degeneration and its deficiency promotes healing after needle puncture injury in mice. *Cell Death Dis*. 2019;*10*:754.

31. Pfirrmann CW, Metzdorf A, Zanetti M, Hodler J, Boos N. Magnetic resonance classification of lumbar intervertebral disc degeneration. *Spine*. 2001;*26*:1873-1878.

32. Dutta S, Sengupta P. Men and mice: relating their ages. *Life Sci*. 2016;*152*:244-248.

33. Skaf GS, Ayoub CM, Domloj NT, Turbay MJ, el-Zein C, Hourani MH. Effect of age and lordotic angle on the level of lumbar disc herniation. *Adv Orthop*. 2011;*2011*(950576):1-6.

34. Tam V, Chan WCW, Leung VYL, et al. Histological and reference system for the analysis of mouse intervertebral disc. *J Orthop Res*. 2018;*36*:233-243.

35. Sivan SS, Wachtel E, Roughley P. Structure, function, aging and turnover of aggrecan in the intervertebral disc. *Biochim Biophys Acta*. 2014;*1840*:3181-3189.

36. Zhao C-Q, Zhang YH, Jiang SD, Li H, Jiang LS, Dai LY. ADAMTS-5 and intervertebral disc degeneration: the results of tissue immunohistochemistry and in vitro cell culture. *J Orthop Res*. 2011;*29*:718-725.

37. Alvarez-Garcia O, Matsuzaki T, Olmer M, et al. FOXO are required for intervertebral disk homeostasis during aging and their deficiency promotes disk degeneration. *Aging Cell*. 2018;*17*:e12800.

38. Mathur A, Pandey VK, Kakkar P. PHLPP: a putative cellular target during insulin resistance and type 2 diabetes. *J Endocrinol*. 2017;*233*:R185-R198.

39. Jackson TC, Verrier JD, Semple-Rowland S, Kumar A, Foster TC. PHLPP1 splice variants differentially regulate AKT and PKCα signaling in hippocampal neurons: characterization of PHLPP proteins in the adult hippocampus. *J Neurochem*. 2010;*115*:941-955.

40. Le Maitre CL, Pockert A, Buttle DJ, Freemont AJ, Hoyland JA. Matrix synthesis and degradation in human intervertebral disc degeneration. *Biochem Soc Trans*. 2007;*35*:652-655.

41. Mattson AM, Begun DL, Molstad DHH, et al. Deficiency in the phosphatase PHLPP1 suppresses osteoclast-mediated bone resorption and enhances bone formation in mice. *J Biol Chem*. 2019;*294*:11772-11784.

42. Hwang SM, Feigenson M, Begun DL, et al. Phlpp inhibitors block pain and cartilage degradation associated with osteoarthritis. *J Orthop Res*. 2018;*36*:1487-1497.

43. Sudo H, Minami A. Caspase 3 as a therapeutic target for regulation of intervertebral disc degeneration in rabbits. *Arthritis Rheum*. 2011;*63*:1648-1657.

44. Chen B, Van Winkle JA, Lyden PD, Brown JH, Purcell NH. PHLPP1 gene deletion protects the brain from ischemic injury. *J Cereb Blood Flow Metab*. 2013;*33*:196-204.

45. Brognard J, Sierecki E, Gao T, Newton AC. PHLPP and a second isoform, PHLPP2, differentially attenuate the amplitude of Akt signaling by regulating distinct Akt isoforms. *Mol Cell*. 2007;*25*:917-931.

46. Itsuji T, Tonomura H, Ishibashi H, et al. Hepatocyte growth factor regulates HIF-1α-induced nucleus pulposus cell proliferation through MAPK, PI3K/Akt, and STAT3 mediated signaling. *J Orthop Res*. 2020;*39*:1184-1191. doi:10.1002/jor.24679

47. Kuai J, Zhang N. Upregulation of SIRT1 by Evodiamine activates PI3K/AKT pathway and blocks intervertebral disc degeneration. *Mol Med Rep*. 2022;*26*:265.

48. Liu Q, Tan Z, Xie C, Ling L, Hu H. Oxidative stress as a critical factor might involve in intervertebral disc degeneration via regulating NOXs/FOXOs. *J Orthop Sci*. 2021;S0949-2658(21)00338-9. doi:10.1016/j.jos.2021.09.010

49. Lee KI, Choi S, Matsuzaki T, et al. FOXO1 and FOXO3 transcription factors have unique functions in meniscus development and homeostasis during aging and osteoarthritis. *Proc Natl Acad Sci U S A*. 2020;*117*:3135-3143.

50. Bradley EW, Carpio LR, Newton AC, Westendorf JJ. Deletion of the PH-domain and leucine-rich repeat protein phosphatase 1 (Phlpp1) increases fibroblast growth factor (Fgf) 18 expression and promotes chondrocyte proliferation. *J Biol Chem*. 2015;*290*:16272-16280.

51. Castillejo Becerra CM, Mattson AM, Molstad DHH, et al. DNA methylation and FoxO3a regulate PHLPP1 expression in chondrocytes. *J Cell Biochem*. 2018;*119*:7470–7478.

APPENDIX

TABLE A1 Respective *p-values* of assays an age or sex

	Age (p-values)			Sex (p-values)		
	Interaction	Genotype	Age	Interaction	Genotype	Sex
KRT19	0.237	0.060	*0.002	0.245	*0.015	0.395
Aggrecan	*0.033	0.145	*<0.0001	0.708	*0.017	0.407
ADAMTS5	0.158	*0.018	0.100	0.783	*0.001	0.525
TUNEL	*0.027	0.053	*<0.0001	*0.012	*0.020	*0.001
FoxO1	*0.003	0.531	*0.002	0.335	*0.021	0.361
FoxO3	0.493	0.780	0.164	*0.030	0.506	0.807

Asterisks denote significance.

TABLE A2 IVD degeneration scores

WT												KO											
Female (6 months)			Male (6 months)			Female (20 months)			Male (20 months)			Female (6 months)			Male (6 months)			Female (20 months)			Male (20 months)		
Mouse	Level	Score	Mouse	Level	Score	Mouse	Level	Score	Mouse	Level	Score	Mouse	Level	Score	Mouse	Level	Score	Mouse	Level	Score	Mouse	Level	Score
1	3–4	0	1	3–4	0	1	3–4	4	1	3–4	1.8	1	3–4	0	1	3–4	0	1	3–4	1	1	3–4	4
	4–5	0		4–5	0		4–5	5.3		4–5	1		4–5	0		4–5	0		4–5	7		4–5	5.3
	5–6	0		5–6	0	2	3–4	1	2	3–4	2.7		5–6	0		5–6	0	2	3–4	1	2	3–4	1
			2	3–4	0		4–5	1		4–5	1.7	2	3–4	0	2	3–4	0		4–5	1		4–5	1
				4–5	0	3	3–4	9.2	3	3–4	1.5		4–5	0		4–5	0		5–6	1	3	3–4	9.2
				5–6	0		4–5	1		4–5	1.7		5–6	0		5–6	0	3	3–4	5		4–5	1
			3	3–4	0	4	3–4	2.5	4	3–4	4.2								4–5	1	4	3–4	2.5
				4–5	0		4–5	1		4–5	1								5–6	1		4–5	1
				5–6	0	5	3–4	1.3		5–6	1							4	3–4	2.2	5	3–4	1.3
							4–5	1	5	3–4	14								4–5	1		4–5	1
										4–5	14.3								5–6	1			
									6	3–4	2.7							5	3–4	5.7			
										5–6	15.5								4–5	1.2			
																		6	3–4	2.5			
																			4–5	1			
																		7	3–4	1			
																			4–5	4			
																			5–6	1			
																		8	3–4	1			
																			4–5	1			